Damping Wrist Joint Tremors with Low Cost Soft Robotic

Thien Le, Benoit Auclair, Klara Tomašković, Jose Garcia-Higuera
Technische Universität München - Human-centered Neuroengineering: Neurorehabilitation
Munich, Germany

***Abstract*—Hand tremor attenuation with soft robotics has proven to provide promising results in tremor damping. However, the technology behind these soft robotic solutions is often difficult to replicate beyond well-equipped laboratories and therefore may not be readily accessible to users. This report proposes a novel, low cost soft robotic damping mechanism that can be easily replicated in any university laboratory and that can be integrated to other technologies. Our wrist damping device is light, portable, human-centered, and only weighs 280g. The device's active damping reduces by 48% the energy of a tremor when artificially elicited in subjects through transcutaneous electrical nerve stimulation (TENS) ($t(11) = 4.513, p < 0.0034$). During the nine-hole peg test, subjects have performed faster when the tremors are damped, but no significant effect could be demonstrated with a rejection rate of 5% ($t(9) = 2.128, p < 0.056$).**

***Index Terms*—Tremor damping, intentional tremor, gyroscope, wrist exoskeleton, neurorehabilitation, human-centered robotics.**

I. Introduction

In Parkinson's disease, malfunctioning of dopaminergic neurons leads to an inability to control and coordinate body movements [1]. This condition is chronic and tends to worsen over time. For many patients, this can lead to total disability [2]. The characteristics of tremors (frequency, amplitude) usually vary over time and depend on the task being carried out [3]. Tremors are divided into 2 categories: resting tremors or action tremor [4].

Among the different approaches aiming at an attenuation of the tremors, [5] has proposed a soft damping mechanism based on viscoelastic fluid activated by a magnetic signal, which inspired the system presented in this report. The main symptoms our system targets are the tremors that are characteristic of medical conditions such as Parkinson's disease, essential tremor, dystonia, and senile tremor. Our system provides a solution for tremors experienced at the wrist joint and decreases kinetic tremors for extension and flexion, a subset of action tremor. The use case for the device is an individual reaching an object and attenuate the tremor that may be present during this action. The device detects when a tremor is present and actuates the damping mechanism accordingly. In that regard, since it discriminates voluntary movement from tremor, the device also is usable for rest tremor.

II. Background

Zahedi et al. [5] outlines a solution to attenuate tremors in the wrist. The specific technology (viscoelastic fluid activated by magnetic signals) being used is however out of our reach. Their research nevertheless provides good input to our project as far as the mechanical components and prosthesis are concerned.

Bhavana et al. [1] provides an implementation of a tremor-detection system relying on IMU sensors. The research shows clear benefits for the use of IMUs over the more widespread use of EMGs in the clinical field. Our system will be using IMU signals to detect whether the tremor has been dampened or is allowed to go through.

Rocon et al. [2] describes the design and validation of a Rehabilitation Robotic Exoskeleton for Tremor Assessment and Suppression. The research builds upon the tremor estimation algorithm established by Riviere [6], weighted-frequency Fourier linear combiner. Based on the frequency distinction between volitional movement and tremors, a harmonic function is fitted to scattered measured data from the accelerometer, thus extracting tremor motion. Two control strategies for tremor damping are outlined, tremor reduction through impedance control, and notch filtering at tremor frequency and applying the opposite force. We will consider those control strategies as a possible starting point for the control algorithm in our system.

III. Methods

A. Exoskeleton design

The exoskeleton consists of 2 separate parts that sit on the hand and on the forearm. Each of them has an inner lining of soft fabric and is fixed to the user's body with stretchable hook-and-loop fasteners. The hand exoskeleton shown in Figure (1 has a bottom part 3D-printed with flexible TPU material to allow the side wings to make close contact with the user's body and provide a better fit. The bottom part is glued to its top, rigid part that houses the IMU sensors and the pin of the actuator described below.

The wrist exoskeleton is entirely 3D-printed with PLA material and thus rigid. It is composed of a bottom part that matches the geometry of the forearm and of a top part with its inside compartmentalized to house the rest of the components (battery, processing unit, servomotor, potentiometer, 9-to-5 V converter). This exoskeleton is closed with a removable lid that hides and protects the electronics (Figure 2). A side opening gives access to a potentiometer and the device switch. The potentiometer allows the user to adjust the set point of the controller and therefore vary the level of dampening as desired.

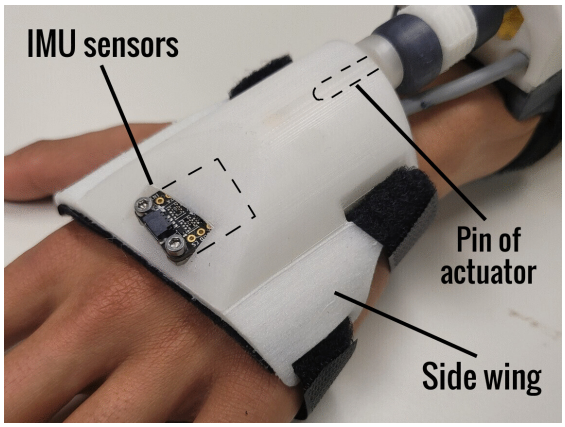

Fig. 1. Exoskeleton of the hand. The dashed lines illustrate the contours of the components inside the exoskeleton.

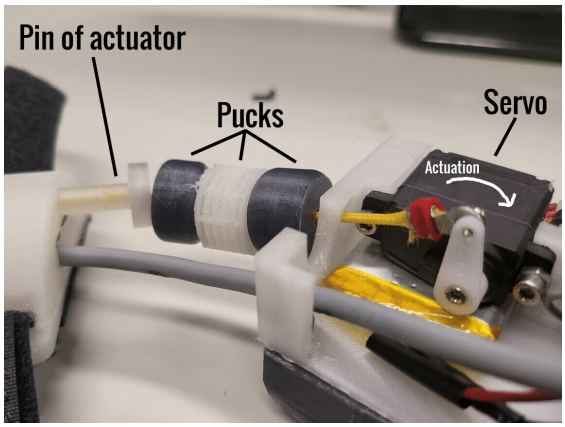

Fig. 3. Soft actuation mechanism. Gradual tightening of the string increasingly dampens the tremors.

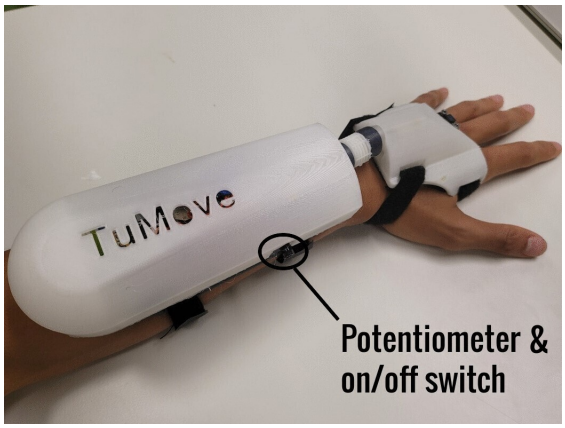

Fig. 2. Whole assembly of the prototype fixed to the user's arm.

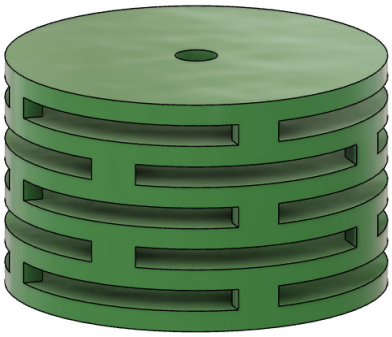

Fig. 4. The mechanical design of the middle puck and its manufacturing with 3D-printed flexible TPU makes it compressible and allows for a smoother damping.

The hand and wrist exoskeletons are united by a soft actuation mechanism that does not constrain the wrist joint's natural degrees of freedom when the device is not active. This mechanism is made up of 2 rigid pucks on either side of a compressible puck, a pin that locks in the hand exoskeleton, a string that runs through all of them and pulls this stack against the forearm exoskeleton when the servo is actuated. If tremors are present and the device is on, the string is gradually tightened and the system reduces the wrist's degree of freedom down to a single translation along the forearm's length (Figure 2).

B. Tremor sensing

An IMU system (ICM-20948 9-DoF) is located on the hand and used to measure the tremor at the wrist. The sensor is integrated on an Adafruit PCB with dimensions 25.7mm x 17.7mm x 4.6mm. The board is oriented so that the IMU's Y-axis is approximately normal to the plane of flexion and extension motions. The signals from the IMU are processed by HUZZAH32 - ESP32 Feather, a system on a chip microcontroller with integrated Wi-Fi. This control system is responsible for signal acquisition, processing as well as actuator control.

We analyze the performance of the accelerometer and of the gyroscope for different axes to report on the absence or on the presence of tremors during TENS stimulation. Both showed oscillatory behavior when TENS stimulation was on, however gyroscope data showed less drift and higher amplitude oscillations, especially for the Y axis (perpendicular to flexion/extension movement). Hence, we decided to use the Y axis of the gyroscope data in the control mechanism. The maximum gyroscope sampling frequency was set to 40Hz and the angular velocity to $\pm 250°/s$.

C. Damping strategy

The first stage of the signal processing pipeline is the Discrete Fast Fourier Transform (DFT) on the gyroscope signal. As human motion is contained in the frequencies 0-20 Hz [7], we gyroscope date is sampled at a frequency of 40 Hz in line with the sampling theorem. To keep the balance between frequency resolution and computational efficiency, the DFT is computed over 16 samples, which resulted in a frequency resolution of 2.5 Hz. Preliminary tests showed when the TENS stimulation is done at 10 Hz, its energy is mostly contained in the frequency bands between 7.5 and 12.5 Hz.

In a second step the root mean square (RMS) of the energy of the spectrum in the range 7.5 to 12.5 Hz is computed.

However, we do not try to control this variable directly because sudden voluntary motion causes spikes in this range. The energy increase caused by tremors persists during a longer period which allows for discrimination between tremor and voluntary movement when averaged over multiple samples. The ideal number of samples avoids unnecessary responses to motions which are not the consequence of tremor stimulation and optimizes the computation time. Based on these requirements, an adequate averaging is achieved with 5 samples from the DFT. In summary, the formula used to calculate tremor energy at each iteration is:

$$E_T[n] = \frac{1}{W}\sqrt{\sum_{k=0}^{W-1}\frac{1}{B^2}\left(\sum_{f\in f_T} X_{n-k}^2(f)\right)}$$

where E_T is the tremor energy in the nth sampling period, W is the number of samples for the RMS operation across different sampling periods, $n-k$ indicates the index of the sampling period, with $k=0$ corresponding to the current one. $X_{n-k}(f)$ is the output of the Fourier transform at a frequency f for the sample period $n-k$. Set f_T is the set of frequencies considered in the control scheme, and B is the number of frequencies contained within that set ($B = card(f_T)$). For our application, $W = 5$ and $f_T = \{7.5, 10, 12.5\}$.

The damping mechanism utilizes a PD (proportional and differential to the error) control scheme. PD control has the benefits of simplicity and robustness. This follows the team's vision of 'user friendly', applicable for both main user and therapy team. Therefore, future adjustment to the controller can be easily made. The control scheme is outline as:

$$e_n = u_n - \mathcal{E}_{n-1}$$

$$m_n = k_p * e_n + k_d\frac{e_n - e_{n-1}}{\delta t}$$

where $\mathcal{E}$ is the tremor energy detected from the IMU (RMS over 5 sampling periods, as described previously), u_n is the user's input from the potentiometer,m_n is the motor command output of the controller, e_n is the value of the error, kp and kd are the proportional and derivative gains respectively, n represents the corresponding variable at the n^{th} sampling instant.

D. Circuit integration

The final circuit is presented in the Figure 5. The IMU is connected to the ESP32 board, which is connected to the servomotor. The power supplies for the acquisition system and the servo motor are different because of different voltage requirements and to be able to provide sufficient current to the servo without affecting the processing unit. A buck converter was used to lower the voltage of a 9V battery to 5V which was the voltage required by the servo motor.

E. Tremor analysis and data acquisition

To simulate tremors we used a Transcutaneous Electrical Nerve Stimulation (TENS), manufactured by Axion, model STIM-PRO X9+. The device transmits electrical impulses via the electrodes through the skin, which can then cause muscle contractions. The intensity of the stimuli can be adjusted between 0 and 100, and the frequency is adjustable between 2Hz and 150Hz [8]. We chose a frequency of 10 Hz for our tests, which is within the range of the frequencies typically associated with tremors [9]. In the initial tests, the electrodes were placed at different locations along the forearm to find the optimal place to simulate wrist tremors. The aim was to find the position that would affect flexion and extension movements the most, i.e. to generate the greatest number of changes in the axis perpendicular to wrist flexion and extension. Figure 6 shows the final location of the electrodes.

F. Experimental evaluation

To assess the effectiveness of the device, 2 experiments were performed. Five participants (healthy, age 22-36) consisted of 4 members of the team and 1 external participant. We explained the testing procedure to each participant, who had time to get accustomed to the TENS electrical stimulation on their left arm. All participants agreed verbally to complete the tests. Then, team members assisted the participants to put on the exoskeleton on their left arm and performed a final fit check. Participant kept the exoskeleton on for the whole duration of the tests. The TENS intensity is set at 26, its rate at 10Hz, with a pulse width of 100μs. One participant had excessive muscular damping of the stimulation; therefore, the team increased the stimulation intensity to 36 to produce a more defined tremor.

Experiment 1 - Damping Mechanism Test: Participants find comfortable position in the chair with their elbow rested on the table. For this test, the exoskeleton was connected to a PC for Serial data readout. The trial began shortly before the team turns on the TENS. This undamped posture is maintained for 5 seconds. Subsequently, the exoskeleton's damping function is turned on manually by a team member. This damped posture is maintained for 5 seconds. The data (energy within the tremor frequency bands and its RMS over 5 sampling periods, setpoints for the controller and the angle output to the servo motor) is recorded throughout the trial. Each posture is performed three times. One participant dropped out of this test due to a bicycle accident.

Experiment 2 - Functional Test: To further assess the damping capability of the exoskeleton, the 9-hole-peg-test (Figure 7) is used to quantify more natural and dynamics movements. Each participant iteratively goes through the peg test while wearing the device under the following conditions: without tremor, tremor with no damping, and tremor with damping. Rest of 1 minute was given between each condition. Completion time of each trial is recorded, and each participant completes 2 trials.

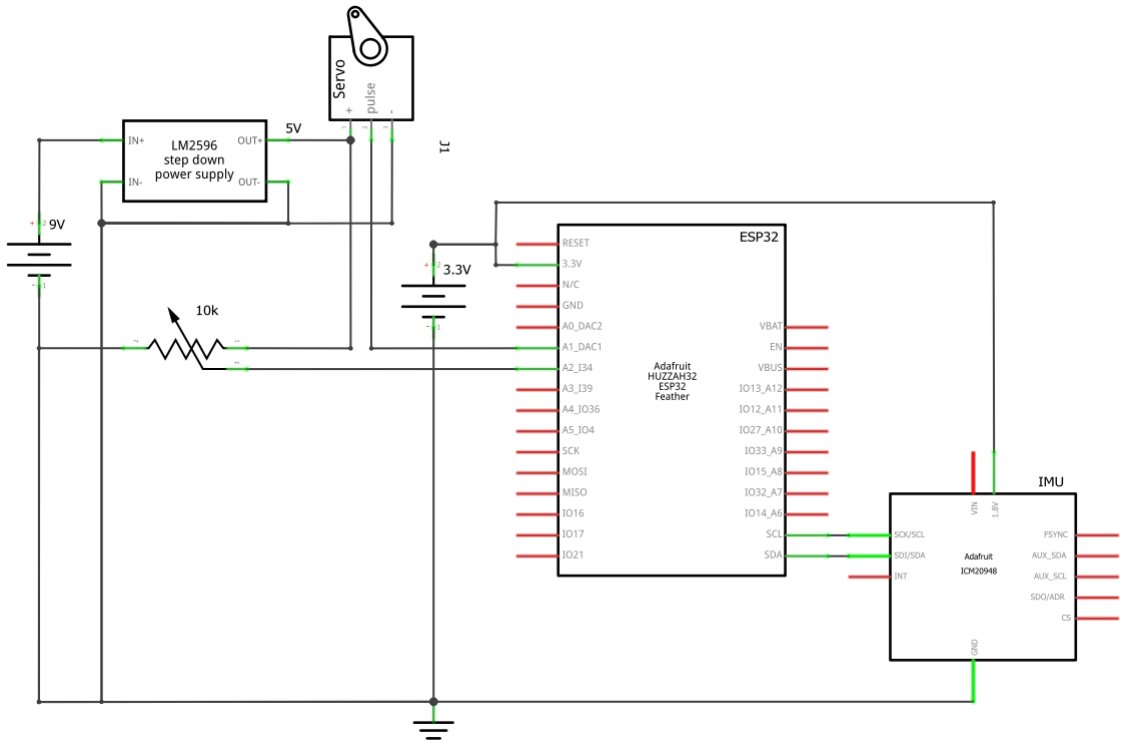

Fig. 5. Circuit schematic.

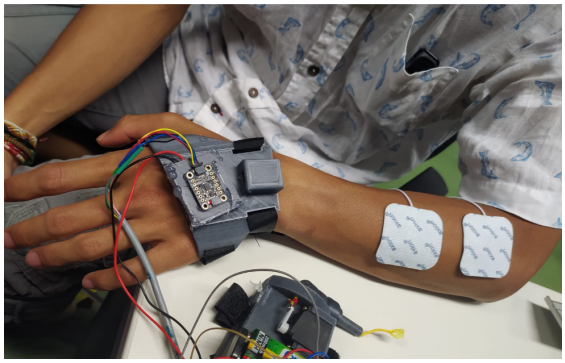

Fig. 6. TENS electrodes position for tremor simulation

IV. Results

In order to assess the extent to which the device dampens the tremor, we ran *Experiment 1* during which the subject's elbow rests on the table and the forearm hangs in the air at rest. Four subjects participated and completed 3 trials each. Figure 8 shows one trial from beginning to end. The beginning of the trial shows close to 0 energy in the tremor frequency band as the TENS stimulation is off. The energy subsequently increases when the TENS stimulation is turned on. At this point, the dampening mechanism is still not activated to observe the effect of stimulation. As set point to the controller (red curve in Figure 8) is lowered below the current energy level, actuation and damping begins (black curve), and the energy decreases in the tremor frequency range.

Fig. 7. 9-Hole-Peg-Test Setup

The trial illustrated in Figure 8 was repeated 12 times overall and the mean energy was calculated over a window of 20 samples before and after damping was effected. The results are reported in Figure 9. For most subjects the levels of energy varied substantially across trials even though the intensity of

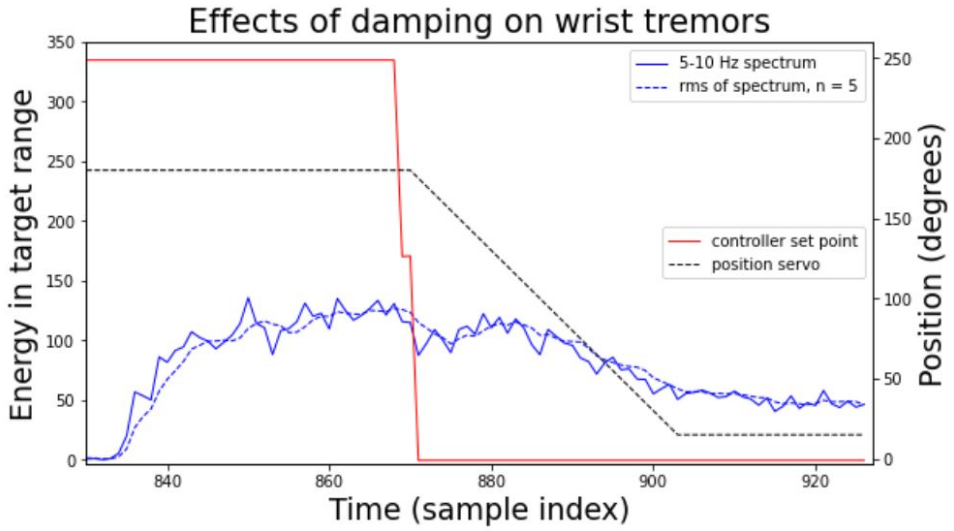

Fig. 8. Data from one subject and one trial: power computed by the DFT in the band 7.5-12.5 Hz (solid blue line), and rms of this power over a window of 5 samples (dashed blue line). The rms of this power is the controlled variable. The level of damping (solid red line) is the set point of the controller. Its setting moves from no damping to complete damping at sample index 870. The position of the servo (dashed black line) indicates the actuation that ensues. The blue lines show a decrease in the tremors once the actuation is effected.

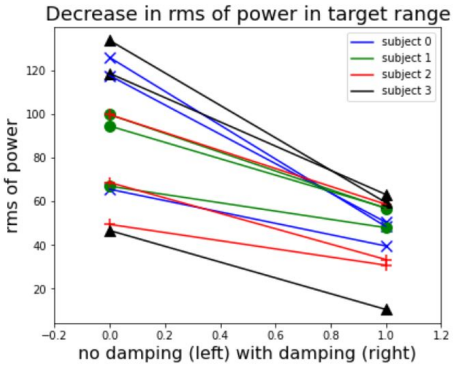

Fig. 9. Data for all 4 subject and 3 trials supports the hypothesis that the device has an impact on the level of tremors experienced by the subject.

Subject	Trial	Baseline[s]	Not dampened[s]	Dampened[s]
A	1	24	29	27
A	2	23	30	28
B	1	25	30	28
B	2	22	22	26*
C	1	25	38	28
C	2	22	24	22
D	1	22	36	27
D	2	23	30	24
E	1	25	36	27
E	2	24	26	26
AVERAGE	-	23.5	30.1	26.3

*Participant reported fatigue

TABLE I
TASK DURATION (SECONDS) FOR ALL SUBJECTS AND ALL TRIALS DURING EXPERIMENT 2.

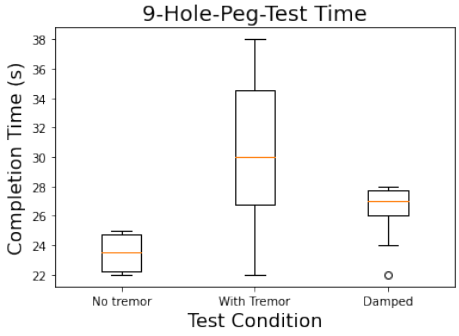

Fig. 10. Functional 9-Hole-Peg-Test

the stimulation was kept constant. This might be the result of displacement of electrodes, habituation to the stimulation, or muscle fatigue. If we disregard this and analyze the relative change in energy in each trial, the mean decrease across all subjects and all trials is 48.2%. The t-test performed on these two conditions supports a significant effect of damping (t-score(11): 4.513, $p < 0.0034$).

The task completion time from the *Experiment 2* (Functional test) is recorded in Table I. Under normal distribution assumption, Welch's test were performed on the 3 conditions of the Functional test, with the rejection significant level of 5%. The results of the test are: no tremor vs tremor (t-score(9) = -3.829, $p < 0.0034$), no tremor vs damped (t-score(9) = -3.810, $p < 0.0017$), tremor vs damped (t-score(9) = 2.128, $p < 0.056$). We conclude that there are significant different in time completion time between no tremor stimulation and with tremor stimulation. However, we cannot draw a definitive significant difference between damped condition and undamped condition, despite being quite close. The team suspected that with higher number of participants, the damping would be significant.

V. Discussion

The device provided quantifiable tremor damping to users. Participants reported noticeable wrist damping in flexion and reflection direction. However, there is no damping at the fingers. The test is done with healthy subjects with tremor stimulation.The TENS artificial tremor is convenient to simulate tremors on healthy subjects; however, there are some inherent problems with this artificial tremor. First, the participant could have introduced bias to the result by overcoming the tremor with muscle contraction. Second, the electrical pulses from the TENS cause muscle fatigue and muscle cramp, reported by participants.

While the device is fully portable, it could be further optimized and made more compact with better power management, i.e. single power supply. This would reduce the weight and size of the device, giving the user a more comfortable exoskeleton. The result of the project demonstrated its capability to damp tremor. However, future work is needed to improve the exoskeleton's ability to dampen tremor of different intensity. In addition, the results of the tremor damping showed decrease in tremor energy, the team was unable show result progressing in the reverse direction, i.e. energy increase when moving from damped condition to undamped condition. This may be at least partially due to the muscle fatigue after having been stimulated for a prolonged time before switching the damping off.

The puck and string mechanism is proof of concept for a novel soft robotic actuator. This simple concept can be adapted to have different dynamic behaviors based on different puck geometry and material. Since the pucks are modular, complex dynamic of the mechanism can be achieved.

VI. Future of Neurorehabilitation

The future of rehabilitation starts with a change in the diagnosis process. In principle, technological tools and biomarkers will be used to suggest both a quantitative diagnosis and best therapy strategy. The role of the medical staff will be to evaluate the proposals and make adjustments. The teams in charge of suggesting, evaluating, and implementing therapies will be more interdisciplinary: neuroscientists, neuro-engineers, doctors, and therapists. Under this collaboration, rehabilitation robotic technologies will be modular, portable, and easily customizable, with each modular component already having been approved by the medical board. This will allow for quick deployment of the optimal solution for the patients. This customizability will not stop with hardware, but also expand to software. One such example of customizable rehabilitation software are gamification-focused therapies. Gamification is essential for the continuation of therapies, as it helps keeping up with the rehabilitation tasks. Sessions should be adjusted to patients and their progress automatically with minimal medical intervention. Furthermore, deep learning will be present in these processes in the future. This allows the therapy team to reach more patients and provide care for all in need. In the specific case of tremors, it is important to note that certain tremors are pathological and mechanical damping, as was applied in the course of this project, may not be the best rehabilitation strategy. For these cases in the future, electrical stimulation directly in the peripheral nervous system may be a valid option as shown by Pascual-Valdunciel et al. [10]. In these cases, robotic intervention would not be necessary.

VII. Human-Centered Engineering

The system in this project was designed following three main approaches: Safety, Comfort and Aesthetics.

Safety: The exoskeleton has safety features in both software and hardware. The servomotor has a stop safety range. Pin of actuator linkage is friction based for possible detachment in case of catastrophic failure, so the the wrist part of the exoskeleton can be detached from the arm part, avoiding extreme extension.

Comfort: After 3 different prototyping iterations, the final prototype has a natural curve for hand and arm comfort. Certain parts were printed in flexible material,so as to have a more user-friendly product. Furthermore, soft material interface is implemented to avoid hard surface contact. The size of the device and its batteries make it a portable and one-package device. The user can manually adjust the intensity of the damping for greater comfort.

Aesthetics: The final prototype seeks to avoid the exposure of any electronic component. In addition, the design aims for elegant, enticing the user to wear it proudly, instead of hiding it under clothes.

VIII. Conclusion

During this project, a prototype exoskeleton with wrist tremor damping (specifically for flexion and extension) was developed. This device was designed with a human-centered approach, prioritizing comfort, safety, portability and appearance. A novel puck and string soft robotic mechanism showed adequate damping. The final prototype weights 280g, and capable of damping up to 48% of the tremor energy in real time. Experiment results on healthy participants showed promising results, but without achieving complete tremor damping during a functional task.

IX. Appendix

The code of the implementation could be found in the following link: https://bit.ly/3bfgymn

References

[1] C. Bhavana *et al.*, "Techniques of measurement for parkinson's tremor highlighting advantages of embedded imu over emg," 2016.

[2] E. Rocon *et al.*, "Design and validation of a rehabilitation robotic exoskeleton for tremor assessment and suppression," *IEEE Transactions on Neural Systems and Rehabilitation Engineering*, vol. 15, 2007.

[3] E. Ohara *et al.*, "Tremor suppression control of meal-assist robot with adaptive filter," 2009.

[4] N. I. of Neurological Disorders and Stroke, "Tremor fact sheet," https://www.ninds.nih.gov/health-information/patient-caregiver-education/fact-sheets/tremor-fact-sheet, 2021, [Online; accessed 25-July-2022].

[5] A. Zahedi *et al.*, "A soft exoskeleton for tremor suppression equipped with flexible semiactive actuator."

[6] C. N. Riviere, R. S. Rader, and N. V. Thakor, "Adaptive cancelling of physiological tremor for improved precision in microsurgery," *IEEE Transactions on Biomedical Engineering*, vol. 45, pp. 839–846, 1998.
[7] D. M. Karantonis *et al.*, "Implementation of a real-time human movement classifier using a triaxial accelerometer for ambulatory monitoring," *IEEE Transactions on Information Technology in Biomedicine*, vol. 10, 2006.
[8] Axion, "Axion stim-pro x9+ instruction manual," https://axion.shop/media/pdf/d8/a6/19/axion-STIM-PRO-X9-PLUS-EN.pdf, [Online; accessed 27-July-2022].
[9] A. Yi *et al.*, "A novel exoskeleton system based on magnetorheological fluid for tremor suppression of wrist joints," *IEEE Int Conf Rehabil Robot.*
[10] A. Pascual-Valdunciel *et al.*, "Peripheral electrical stimulation to reduce pathological tremor: a review," 2021.